

# Topological Entanglement in TQFTs

Hung-Hwa Lin

Department of physics, University of California, San Diego

## Abstract

We discuss the computation of entanglement entropy of topological quantum field theory using axioms in TQFT, which renders such usually difficult calculation in quantum field theories tractable. The basic idea is illustrated, and some examples are given.

## 1 Introduction

Entanglement entropy of quantum field theories, where there are infinite number of degree of freedom, can be difficult to compute and may be sensitive to UV cutoff. However, for topological field theories, such as Chern Simons theory, there exist powerful tools that render calculation tractable. Moreover, from their topological nature, the “area law” terms naturally vanish, and all we obtain is the topological entropy terms. They have been applied to Chern Simons theory to compute bipartite [3] and multipartite [2] entanglement, as well as to (3+1)d topological order described by Dijkraaf-Witten theories [6], all of which utilize the ideas of TQFT[1] and surgery of manifolds [7].

In Section 2, we discuss the basic idea of computing the von-Neumann entropy using techniques of TQFT, and in Section 3 we present some examples.

## 2 Entanglement of TQFTs

In this section, we illustrate the basic idea of using manifolds to compute entanglement in TQFTs. We will see that, after a manifold representing the density matrix  $\rho$  is constructed, the rest is not so different from the TQFT operations discussed in the lecture notes.

### 2.1 Density matrix and the replica trick

In the lectures we have learned that a state of a TQFT can be represented by a manifold with a boundary, or more specifically the path integral on



Figure 1: A manifold with a boundary represents a state  $|\psi\rangle$  [5].



Figure 2: The density matrix  $\rho = |\psi\rangle\langle\psi|$ .

this manifold. For example, something like For entanglement entropy, we normally divide the space into region  $A$ , and  $B$ , reflected on the boundary of the manifold. To form a density matrix from this pure state  $|\psi\rangle$ ,

$$\rho = |\psi\rangle\langle\psi|, \quad (1)$$

is basically formed by two copies of the manifold, one of which with inverted orientation, as shown in Fig. 2. The reduced density matrix <sup>1</sup>

$$\rho_A = \text{tr}_B \rho \quad (2)$$

is then gluing the  $B$  region of the two boundaries in 2 together, so that now the  $\rho_A$  manifold is no longer disjoint unions of two parts, such as in Fig. 3. Lastly,

<sup>1</sup>Note that this is actually the unrenormalized density matrix. To restore unit trace, one should include a factor of  $\text{tr}_A \rho_A$ .

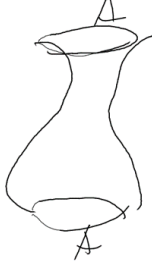


Figure 3: The reduced density matrix  $\rho_A$ .

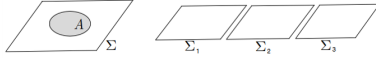


Figure 4: Bipartite (left) and multipartite (right) entanglement [3].

one use the replica trick,

$$S_A = -\frac{\text{tr}\rho_A^n - 1}{n-1}, \quad (3)$$

where  $\rho_A^n$  is then evaluated by gluing  $n$  copies of 3, which after the trace becomes a closed manifold. Some elementary exercises of forming the final manifold of entropy can be found in [5]. A more formal account, addressing the underlying path integral, is in [3] and reviewed in Appendix.A.

## 2.2 Computing the path integral

To actually compute the path integral of  $\rho_A^n$  manifold, possibly complicated, we can use the formula of connected sum [7]

$$Z(M)Z(S^3) = Z(M_1)Z(M_2) \quad (4)$$

for  $M = M_1 \# M_2$  to decompose  $M$  into simpler manifolds. In particular, we've computed  $Z(S^2 \times S^1; \{R_a\})$  in lectures, and then used surgery to compute  $Z(S^3)$ .

## 3 Examples

In this section we show some examples of entanglement entropy of Chern-Simons theory on various spatial surface and partitions, including bipartite entanglement [3] and multipartite entanglement, where the space is partitioned into several disconnected segments, as shown in Fig.

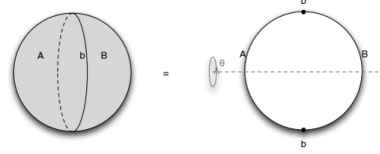


Figure 5: A state with spatial slice  $S^2$  as a boundary of a 3-ball, with hemisphere regions  $A$  and  $B$  [3].

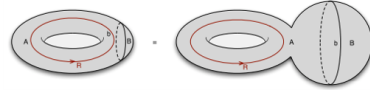


Figure 6: A solid torus with boundary  $T_2$  and partitions  $A$  and  $B$  [3].

## 3.1 Bipartite entanglement

### 3.1.1 $S^2$ with a connected interface

For the simplest case, consider the spatial slice is  $S^2$ , and the regions  $A$  and  $B$  are the two hemispheres, as shown in Fig. 5. . We have learned that the Hilbert space is one-dimensional for a surface  $S^2$ . Then we have  $|\psi\rangle = B^3$ ,  $\rho_A = B^3$ , and  $\text{tr}\rho_A^n = S^3$  for all  $n$ . We thus have

$$\frac{\text{tr}\rho_A^n}{(\text{tr}\rho_A)^n} = \frac{Z(S^3)}{(Z(S^3))^n} = (Z(S^3))^{1-n}, \quad (5)$$

and

$$S_A = \ln [Z(S^3)]. \quad (6)$$

### 3.1.2 Torus with one-component boundary

If instead the spatial slice is a torus and the partition  $A$  and  $B$  are as shown in Fig. 6. Unlike  $S^2$ , the Hilbert space of a torus is not one dimensional. Each state corresponds to an integrable irrep  $R_i$  of the gauge group  $G$ , represented by a solid torus with a Wilson loop  $R_i$  inserted. Then the  $\rho_A^n$  would be an  $S^3$  attached with  $n$  copies of  $S^2 \times S^1$ , as shown in Fig. 7 Note that pairs of solid tori get glued together along with its Wilson loop  $\hat{R}_i$ , so each attached  $S^2 \times S^1$  will contain two Wilson loops  $\hat{R}_i$  and  $\hat{\bar{R}}_i$ , since one of them serves as the “bra” instead of “ket” in

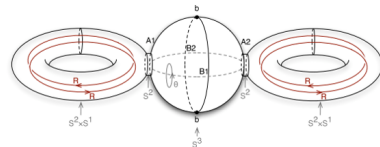


Figure 7: The manifold for  $\rho_A^2$  [3].

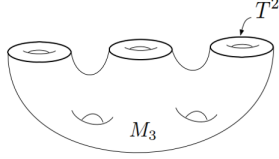


Figure 8: A manifold whose boundary is 3 disjoint tori [2].



Figure 9: The link complement by removing a tubular neighborhood surrounding the 3-component link [2].

the density matrix and gets its orientation reversed. Thus, we have

$$\begin{aligned}
 & \frac{\text{tr} \rho_A^n}{(\text{tr} \rho_A)^n} \\
 &= \frac{1}{Z(S^2 \times S^1, \hat{R}_i, \hat{R}_i)^n} \frac{Z(S^3) Z(S^2 \times S^1, \hat{R}_j, \hat{R}_j)^n}{Z(S^3)^n} \\
 &= Z(S^3)^{1-n}
 \end{aligned} \tag{7}$$

### 3.1.3 Other examples.

Some further examples, where the boundary between  $A$  and  $B$  contains more than one component, can be found in [3], such as those including quasiparticle punctures.

## 3.2 Multipartite entanglement

We may also consider the entanglement between disconnected spatial segments. One of the simplest case is if all these segments are all tori [2]. We would then need to find a 3-d manifold whose boundary is  $n$  disjoint tori, as illustrated in Fig. 8. One way to construct such manifold is by embedding an  $n$ -component link in  $S^3$ , and drill out the tubular neighborhood of each component, called the link complement state, as illustrated in Fig. 9.

This is a case where the wavefunction can be explicitly computed before constructing the density matrix.

Note that the Hilbert space is

$$H = \bigotimes_i H_{T^2, i} \tag{8}$$

is a tensor product of  $n$  Hilbert space of the torus, such link complement state can be expressed as

$$\begin{aligned}
 & |\mathcal{L}^n\rangle \\
 &= \sum C_{\mathcal{L}^n}(j_1, \dots, j_n) |j_1\rangle \otimes \dots \otimes |j_n\rangle,
 \end{aligned} \tag{9}$$

where  $|j_i\rangle$  is the  $j^{\text{th}}$  state of the  $i^{\text{th}}$  torus Hilbert space. It turns out that the wavefunction  $C$  is simply the colored link invariant <sup>2</sup>,

$$\begin{aligned}
 & C_{\mathcal{L}^n}(j_1, \dots, j_n) \\
 &= \left\langle W_{R_{j_1}^*}(L_1) \dots W_{R_{j_n}^*}(L_n) \right\rangle_{S^3}.
 \end{aligned} \tag{10}$$

For example, for gauge group  $U(1)_k$ , we have

$$\begin{aligned}
 & C_{\mathcal{L}^n}(q_1, \dots, q_n) \\
 &= \left\langle W_{-q_1}(L_1) \dots W_{-q_n}(L_n) \right\rangle_{S^3} \\
 &= \exp\left(\frac{2\pi i}{k} \sum_{i < j} q_i q_j \ell_{ij}\right),
 \end{aligned} \tag{11}$$

whre  $\ell_{ij}$  is the Gauss linking number between the components  $L_i$  and  $L_j$ . The density matrix can then be found from  $|\mathcal{L}^n\rangle$ . It turns out that the entropy  $S$  will be non-zero when there is non-trivial linking between the link components.

## 4 Discussion

From these examples we have seen that using the techniques in TQFT, the entanglement entropy of Chern-Simons theory can be reduced to the path integral of some simple manifolds, which in the case of Chern-Simons theory could be computed by conformal field theory, or into some link-invariants, both could be tabulated for reference. One do not need to actually compute the complicated path integral.

One may also reverse the logic and associate physical meaning to the topological invariants. For example, the colored link invariants may be interpreted as the entanglement entropy between disjoint tori space, and even the complexity of computing topological invariants [4].

<sup>2</sup>The idea is this: to compute  $C$ , one takes the inner product of the basis state with the link complement state,  $\langle j_1 \dots j_n | \mathcal{L}^n \rangle$ , which amounts to gluing these  $n$  tori with  $j_i$ -representation Wilson loops glue back to the tubular region originally removed from  $\mathcal{L}^n$ . The resulting manifold is simply the full  $S^3$  with  $n$  component links, so that  $C$  is the link invariant indicated in the formula.

## Acknowledgements

We are grateful for Professor John McGreevy’s course and pointing the direction to references on this topic. To us this is a vast subject that this paper certainly doesn’t do justice for. Most notably the application to (3+1)d topological order was not included, which we hope to do in the future. We also thank En-Jui Kuo for enlightening discussions.

## References

- [1] Michael F Atiyah. Topological quantum field theory. *Publications Mathématiques de l’IHÉS*, 68:175–186, 1988.
- [2] Vijay Balasubramanian, Jackson R Fliss, Robert G Leigh, and Onkar Parrikar. Multi-boundary entanglement in chern-simons theory and link invariants. *Journal of High Energy Physics*, 2017(4):61, 2017.
- [3] Shiyong Dong, Eduardo Fradkin, Robert G Leigh, and Sean Nowling. Topological entanglement entropy in chern-simons theories and quantum hall fluids. *Journal of High Energy Physics*, 2008(05):016, 2008.
- [4] Jackson R Fliss. Knots, links, and long-range magic. *arXiv preprint arXiv:2011.01962*, 2020.
- [5] D Melnikov, A Mironov, S Mironov, A Morozov, and An Morozov. From topological to quantum entanglement. *Journal of High Energy Physics*, 2019(5):1–12, 2019.
- [6] Xueda Wen, Huan He, Apoorv Tiwari, Yunqin Zheng, and Peng Ye. Entanglement entropy for (3+ 1)-dimensional topological order with excitations. *Physical Review B*, 97(8):085147, 2018.
- [7] Edward Witten. Quantum field theory and the jones polynomial. *Communications in Mathematical Physics*, 121(3):351–399, 1989.

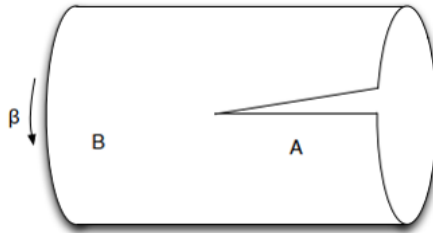


Figure 10: An illustration of  $\rho_A$  corresponding to (??) [3].

## A Path integral representation of the entanglement entropy

To simplify matter, let’s first consider the finite temperature density matrix of a scalar field,

$$\begin{aligned} & \rho [\{\phi_0(\vec{x})\}, \{\phi_\beta(\vec{x})\}] \\ &= \frac{1}{Z(\beta)} \left\langle \{\phi_0(\vec{x})\} \left| e^{-\beta \hat{H}} \right| \{\phi_\beta(\vec{x})\} \right\rangle \\ &= \int \prod_{\vec{x}, \tau} [d\phi(\vec{x}, \tau)] e^{-S_E} \\ & \prod_{\vec{x}} \delta[\phi(\vec{x}, 0) - \phi_0(\vec{x})] \delta[\phi(\vec{x}, \beta) - \phi_\beta(\vec{x})], \quad (12) \end{aligned}$$

which is basically integrating out everything else except for fixing the field configuration at  $\tau = 0, \beta$  as the values  $\phi_0, \phi_\beta$ . To obtain the reduced density matrix  $\rho_A$ , we further integrate out the spatial region  $B$  in  $\tau = 0, \beta$  too,

$$\begin{aligned} & \rho_A [\{\phi_0(\vec{x})\}, \{\phi_\beta(\vec{x})\} | \vec{x} \in A] \\ &= \int \left( \prod_{\vec{x} \in B} [d\phi_0(\vec{x}) d\phi_\beta(\vec{x})] \delta[\phi_0(\vec{x}) - \phi_\beta(\vec{x})] \right) \\ & \rho [\{\phi_0(\vec{x})\}, \{\phi_\beta(\vec{x})\}], \quad (13) \end{aligned}$$

as shown in Fig. 10, where the cut boundary at  $A$  is not integrated. Then the replica  $\text{tr} \rho_A^n$  is obtained from  $n$  copies of  $\rho_A$  and integrating over appropriate fields,

$$\begin{aligned} & \text{tr} \rho_A^n \\ &= \int \prod_{k=1}^n \left\{ \prod_x [d\phi_0^{(k)}(\vec{x}) d\phi_\beta^{(k)}(\vec{x})] \prod_{x \in A} \delta[\phi_0^{(k)}(\vec{x}) - \phi_\beta^{(k+1)}(\vec{x})] \right. \\ & \left. \prod_{x \in B} \delta[\phi_0^{(k)}(\vec{x}) - \phi_\beta^{(k)}(\vec{x})] \rho [\{\phi_0^{(k)}(\vec{x})\}, \{\phi_\beta^{(k+1)}(\vec{x})\}] \right\}, \quad (14) \end{aligned}$$

akin to gluing  $n$  copies of manifolds as shown in Fig. 11 .

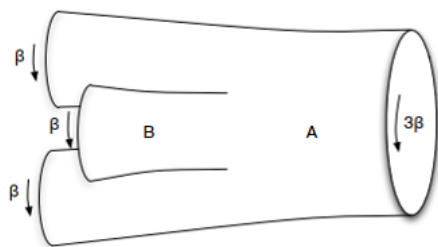


Figure 11:  $\text{tr}\rho_A^3$  obtained by gluing three copies of Fig.10 [3].